

Detecting the cosmic acceleration with current data

Rong-Gen Cai ^{*}, Zhong-Liang Tuo [†]

*Key Laboratory of Frontiers in Theoretical Physics,
Institute of Theoretical Physics, Chinese Academy of Sciences,
P.O. Box 2735, Beijing 100190, China*

Abstract

The deceleration parameter q as the diagnostic of the cosmological accelerating expansion is investigated. By expanding the luminosity distance to the fourth order of redshift and the so-called y -redshift in two redshift bins and fitting the SNIa data (Union2), the marginalized likelihood distribution of the current deceleration parameter shows that the cosmic acceleration is still increasing, but there might be a tendency that the cosmic acceleration will slow down in the near future. We also fit the Hubble evolution data together with SNIa data by expanding the Hubble parameter to the third order, showing that the present decelerating expansion is excluded within 2σ error. Further exploration on this problem is also approached in a non-parametrization method by directly reconstructing the deceleration parameter from the distance modulus of SNIa, which depends neither on the validity of general relativity nor on the content of the universe or any assumption regarding cosmological parameters. More accurate observation datasets and more effective methods are still in need to make a clear answer on whether the cosmic acceleration will keep increasing or not.

PACS numbers:

^{*} Email: cairg@itp.ac.cn

[†] Email: tuozhl@itp.ac.cn

I. INTRODUCTION

More than ten years has passed since two independent groups discovered that our universe entered a stage of accelerating expansion using the Type Ia Supernova (SNIa) data [1]. During the past years, many observations embrace the results, such as large scale structure [2], the cosmic microwave background (CMB) radiation [3], and so on. All of these data strongly suggest that we live in an accelerating universe, with the deceleration parameter $q < 0$ at low redshift, and an exotic component named dark energy is introduced to interpret this phenomena [4]. As more and more observational data released, the cosmic expansion history can be more accurately determined [5, 6].

Besides the eternal acceleration scenario, such as the well-known Λ CDM model, some authors have proposed that a matter dominated decelerating expansion will resume soon after the acceleration starts, because the vacuum energy's anti-gravitational properties will reversed [7]. Using the CPL parametrization [8], Shafieloo et al. [9] recently found that the cosmic acceleration might be slowing down. This question is interesting, since it challenges the Λ CDM model, which fits most of the current data very well and predicts an eternal cosmic acceleration. But this result is far from final judgement. First, different parametrization methods of dark energy equation of state will show different influences on the evolution behavior of the universe [10], and the CPL ansatz might be unable to fit the data simultaneously at low and high redshifts. Second, some tensions also might exist in the SNIa dataset which may lead to different results in the joint analysis [11, 12], with one suggesting a decreasing acceleration, others just the opposite. In order to avoid these disadvantages, one can consider the so-called cosmographic approach [13], by directly parameterizing the deceleration parameter, such as linear expansion $q(z) = q_0 + q_1 z$ [14], or other two-parameter model $q(z) = \frac{1}{2} + \frac{q_1 z + q_2}{(1+z)^2}$ [15]. And some authors discovered that the universe might have already entered a decelerating expansion era by using only low (for example $z < 0.1$ or $z < 0.2$) redshift SNIa data [16, 17].

In this paper, we focus on the deceleration parameter as the diagnostic of the cosmological accelerating expansion. Following the approach introduced in [16], we investigate the deceleration parameter by expanding the luminosity distance to the fourth order of

redshift and the so-called y -redshift [18], and fitting the latest SNIa sample (Union2) released by the Supernova Cosmology Project (SCP) Collaboration [19], which contains 557 data including recent large samples from other surveys and uses SALT2 for SNIa light-curve fitting. But instead of cutting off the data at low redshift, we use the sub-samples with $z < 1.0$ throughout the paper, in order to circumvent the convergence issues discussed in [20] and to make our discussion physically meaningful, while applying some other technique to reduce the accumulation of systematic error, also we introduce some physical constraint conditions to make our constraint more robust [21]. To make an overall comparison, the Hubble parameter $H(z)$ is also expanded to the third order of the redshift and the y -redshift and fitted to the Hubble evolution data [22, 23]. This constitutes the second part of the paper. In Sec. 3, we propose a non-parametrization method to reconstruct the deceleration parameters at different redshifts directly from the SNIa data, and this method is independent of the calibration of the SNIa data. Sec. 4 contains our conclusion.

II. COSMOGRAPHIC EVALUATION

A. Methodology

We adopt the assumption that the universe has a flat Friedmann-Robertson-Walker (FRW) metric and then the scale factor can be approximated by the first several terms in a Taylor series; i.e., as a fifth order polynomial [24]. The coefficients in this expansion are considered as the parameters of the theory. Since one more term taken will greatly reduce the constraint ability of the parameter (see Table 1 in the first paper of [25]) and four-parameter series can give a better approximation to the Hubble parameter and the distance modulus than other expansions [21]. Therefore we take the first four terms only in our analysis.

Accordingly, the luminosity distance $d_L(z)$ can be expanded to the fourth order of

redshift [13, 16, 24], which is a generalized form of the Hubble law,

$$d_L(z) = \frac{1}{H_0} \left[z + \frac{1}{2}(1 - q_0)z^2 - \frac{1}{6}(1 - q_0 - 3q_0^2 + j_0)z^3 \right. \\ \left. + \frac{1}{24}(2 - 2q_0 - 15q_0^2 - 15q_0^3 + 10q_0j_0 + 5j_0 + s_0)z^4 \right] + \mathcal{O}(z^5), \quad (1)$$

where the coefficients are expressed with H_0 , q_0 , j_0 , and s_0 , the present values of Hubble, deceleration, jerk and snap parameters, respectively. This kinematic method can give valuable information regarding the expansion rates of the universe, thus provides us with a testing ground for all cosmological solutions. To circumvent the convergence issues as discussed in [20], we choose the redshift cutoff $z < 1.0$ with 537 SNIa events involved.

A so-called y -redshift is introduced in [20], where $y = \frac{z}{1+z}$. In this case, the luminosity distance can be expanded as

$$d_L(y) = \frac{1}{H_0} \left[y + \frac{1}{2}(3 - q_0)y^2 + \frac{1}{6}(11 - 5q_0 + 3q_0^2 - j_0)y^3 \right. \\ \left. + \frac{1}{24}(50 - 26q_0 + 21q_0^2 - 15q_0^3 + 10q_0j_0 - 7j_0 + s_0)y^4 \right] + \mathcal{O}(y^5). \quad (2)$$

This expansion converges faster than the expansion with the redshift z and the systematic error in this case is much smaller than the former case. This expansion has been extensively studied in [16].

In principle, the luminosity distance d_L at low redshift ($z < 1$) can be exactly expressed by the infinite power series expansion of z or y , yet with infinite parameters involved. In practice, we choose the first four terms of the Taylor series as an approximation, which leads to the truncation error in our analysis. This is considered as the systematic error. The systematic error in (2) is relatively larger compared with the Union2 data. For example, when $y = 1/2$, the systematic error in 2 is about 3.1%, while it is 1.0% in the SNIa data. In order to make the systematic error smaller than that of the Union2 data, one has to cut off the data with $z \geq 0.398$. Here we employ another method to deal with this issue, rather than striking off high- z SNIa data. First, we separate the data ($z < 1.0$) equally in two redshift bins and the divide is $z_{cut} = 0.274$, to guarantee that there are enough data in each bin. And then we employ Eqs. (1) and (2) in each redshift bin, respectively. Note that for the $z > z_{cut}$ case, the luminosity distance can be expanded around $z = \frac{1}{2}$, which separates the data ($0.274 < z < 1$) equally in two parts. This

method will reduce the systematic error and give a better constraint. Accordingly, the luminosity distance for $z > z_{cut}$ can be expressed as

$$\begin{aligned}
d_L(z > z_{cut}) = & \frac{1}{H_0} \left[\frac{1}{24} (2 - 2q_0 - 15q_0^2 - 15q_0^3 + 10q_0j_0 + 5j_0 + s_0) \left(z - \frac{1}{2}\right)^4 \right. \\
& - \frac{1}{6} (1 - q_0 - 3q_0^2 + j_0 - \frac{1}{2} (2 - 2q_0 - 15q_0^2 - 15q_0^3 + 10q_0j_0 + 5j_0 + s_0)) \\
& \left. \left(z - \frac{1}{2}\right)^3 + \left(\frac{1}{16} (2 - 2q_0 - 15q_0^2 - 15q_0^3 + 10q_0j_0 + 5j_0 + s_0) - \frac{1}{4} \right. \right. \\
& \left. \left. (1 - q_0 - 3q_0^2 + j_0) + \frac{1}{2} (1 - q_0) \right) \left(z - \frac{1}{2}\right)^2 + \left(1 + \frac{1}{2} (1 - q_0) \right. \right. \\
& \left. \left. - \frac{1}{8} (1 - q_0 - 3q_0^2 + j_0) + \frac{1}{48} (2 - 2q_0 - 15q_0^2 - 15q_0^3 + 10q_0j_0 + 5j_0 + s_0) \right) \right. \\
& \left. \left(z - \frac{1}{2}\right) \right] + d_L\left(\frac{1}{2}\right). \tag{3}
\end{aligned}$$

Using the y -redshift, the divide is $y_{cut} = 0.215$ and the luminosity distance for the $y > y_{cut}$ case can be expanded around the point $y = \frac{1}{3}$,

$$\begin{aligned}
d_L(y > y_{cut}) = & \frac{1}{H_0} \left[\frac{1}{24} (50 - 26q_0 + 21q_0^2 - 15q_0^3 + 10q_0j_0 - 7j_0 + s_0) \left(y - \frac{1}{3}\right)^4 \right. \\
& + \frac{1}{6} \left(\frac{1}{3} (50 - 26q_0 + 21q_0^2 - 15q_0^3 + 10q_0j_0 - 7j_0 + s_0) \right. \\
& + 11 - 5q_0 + 3q_0^2 - j_0) \left(y - \frac{1}{3}\right)^3 + \frac{1}{2} \left(\frac{1}{3} (11 - 5q_0 + 3q_0^2 - j_0) \right. \\
& + \frac{1}{18} (50 - 26q_0 + 21q_0^2 - 15q_0^3 + 10q_0j_0 - 7j_0 + s_0) + 3 - q_0) \left(y - \frac{1}{3}\right)^2 \\
& + \left(1 + \frac{1}{3} (3 - q_0) + \frac{1}{18} (11 - 5q_0 + 3q_0^2 - j_0) + \frac{1}{162} \right. \\
& \left. \left. (50 - 26q_0 + 21q_0^2 - 15q_0^3 + 10q_0j_0 - 7j_0 + s_0) \right) \left(y - \frac{1}{3}\right) \right] + d_L\left(\frac{1}{3}\right). \tag{4}
\end{aligned}$$

The systematic error of Eq. (4) is about 0.411%, which is comparable with the most accurately detected SNIa data, whose error is 0.212%.

The Hubble parameter $H(z)$ can also be expressed with H_0, q_0, j_0, s_0 by expanding it to the third order. Since $q(z)$ is related to the second order derivative of $d_L(z)$, and the first order derivative of $H(z)$, this expansion is worthwhile to make a full analysis. Using the redshift and the y -redshift, the hubble parameter can be expanded as

$$E(z) \equiv \frac{H(z)}{H_0} = 1 + (1 + q_0)z + \frac{1}{2} (j_0 - q_0^2)z^2 + \frac{1}{6} (3q_0^2 + 3q_0^3 - 3j_0 - 4q_0j_0 - s_0)z^3, \tag{5}$$

and

$$E(y) \equiv \frac{H(y)}{H_0} = 1 + (1+q_0)y + \frac{1}{2}(2+2q_0+j_0-q_0^2)z^2 + \frac{1}{6}(6+6q_0-3q_0^2+3q_0^3+3j_0-4q_0j_0-s_0)y^3. \quad (6)$$

Similarly, in order to reduce the systematic error, we expand the Hubble parameter in the regime of redshift $z > z_{cut}$ as

$$\begin{aligned} \frac{H(z > z_{cut})}{H_0} &= [1 + q_0 + \frac{1}{2}(j_0 - q_0^2) + \frac{1}{8}(3q_0^2 + 3q_0^3 - 3j_0 - 4q_0j_0 - s_0)](z - \frac{1}{2}) \\ &\quad + \frac{1}{2}[j_0 - q_0^2 + \frac{1}{2}(3q_0^2 + 3q_0^3 - 3j_0 - 4q_0j_0 - s_0)](z - \frac{1}{2})^2 \\ &\quad + \frac{1}{6}(3q_0^2 + 3q_0^3 - 3j_0 - 4q_0j_0 - s_0)(z - \frac{1}{2})^3 + \frac{H(\frac{1}{2})}{H_0}, \end{aligned} \quad (7)$$

and

$$\begin{aligned} \frac{H(y > y_{cut})}{H_0} &= [1 + q_0 + \frac{1}{3}(2 + 2q_0 + j_0 - q_0^2) + \frac{1}{18}(6 + 6q_0 - 3q_0^2 + 3q_0^3 + 3j_0 - 4q_0j_0 \\ &\quad - s_0)](y - \frac{1}{3}) + \frac{1}{2}[2 + 2q_0 + j_0 - q_0^2 + \frac{1}{3}(6 + 6q_0 - 3q_0^2 + 3q_0^3 + 3j_0 - 4q_0j_0 \\ &\quad - s_0)](y - \frac{1}{3})^2 + \frac{1}{6}(6 + 6q_0 - 3q_0^2 + 3q_0^3 + 3j_0 - 4q_0j_0 - s_0)(y - \frac{1}{3})^3 \\ &\quad + \frac{H(\frac{1}{3})}{H_0}. \end{aligned} \quad (8)$$

B. Datasets

The dataset we use is the most recently released Union2 SNIa dataset [19], which contains 537 events for $z < 1.0$. We fit the SNIa by minimizing the χ^2 value of the distance modulus and the χ_{sn}^2 for SNIa is obtained by comparing theoretical distance modulus $\mu_{th}(z) = 5 \log_{10}[d_L(z)] + \mu_0$, where $\mu_0 = 42.384 - 5 \log_{10} h$, with observed μ_{ob} of supernovae:

$$\chi_{sn}^2 = \sum_i^{537} \frac{[\mu_{th}(z_i) - \mu_{ob}(z_i)]^2}{\sigma^2(z_i)}$$

To reduce the effect of μ_0 , we expand χ_{sn}^2 with respect to μ_0 [28] :

$$\chi_{sn}^2 = A + 2B\mu_0 + C\mu_0^2 \quad (9)$$

where

$$\begin{aligned} A &= \sum_i \frac{[\mu_{th}(z_i; \mu_0 = 0) - \mu_{ob}(z_i)]^2}{\sigma^2(z_i)}, \\ B &= \sum_i \frac{\mu_{th}(z_i; \mu_0 = 0) - \mu_{ob}(z_i)}{\sigma^2(z_i)}, \\ C &= \sum_i \frac{1}{\sigma^2(z_i)}. \end{aligned}$$

Eq. (9) has a minimum as

$$\tilde{\chi}_{sn}^2 = \chi_{sn,min}^2 = A - B^2/C$$

which is independent of μ_0 . In fact, it is equivalent to performing an uniform marginalization over μ_0 , the difference between $\tilde{\chi}_{sn}^2$ and the marginalized χ_{sn}^2 is just a constant [28]. We will adopt $\tilde{\chi}_{sn}^2$ as the goodness of fit between theoretical model and SNIa data.

In order to discriminate the evolution behaviors of different models, another dataset is also employed, which is the recently summarized Hubble evolution data [22], containing 7 data at redshift $z < 1.0$. We add in three more data at $z = 0.24, 0.34, 0.43$ by taking the BAO scale as a standard ruler in the radial direction [23], and also $H(z = 0) = 74.2 \pm 3.6 (km/(s \cdot Mpc))$ observed by the Hubble Space Telescope (HST) [26]. The χ_H^2 is defined as

$$\chi_H^2 = \sum_{i=1}^{11} \frac{[H(z_i) - H_{ob}(z_i)]^2}{\sigma_i^2}.$$

To make use of the data, we perform a uniform marginalization over the nuisance parameter H_0 and get

$$\tilde{\chi}_H^2 = \chi_{H,min}^2 = a - c^2/b,$$

where

$$\begin{aligned} a &= \sum_i \frac{H_{ob}(z_i)^2}{\sigma^2(z_i)}, \\ b &= \sum_i \frac{[H_{th}(z_i)/H_0]^2}{\sigma^2(z_i)}, \\ c &= \sum_i \frac{H_{ob}(z_i)H_{th}(z_i)/H_0}{\sigma^2(z_i)}. \end{aligned}$$

C. Results

The analysis is performed by using the Monte Carlo Markov Chain in the multidimensional parameter space to derive the likelihood. It is natural to employ some physically obvious limitations to make the estimation of parameters more robust [21]. We impose the positiveness conditions of the Hubble parameter and the luminosity distance when we move randomly in the parameter space, and select the points satisfying these conditions as our chains. Note that these conditions are independent of the content of the universe and the requirement of matter density fraction, In this sense they are robust and the priors are:

$$\begin{aligned} d_L(z) &> 0, \\ H(z) &> 0. \end{aligned}$$

We first investigate the constraint on the model parameters using the SNIa data, and add the Hubble evolution data for a comparison, then we analyze the evolution behavior of the deceleration parameters. The best-fitting values and errors of parameters for $d_L(z)$, $d_L(y)$ and $d_L^{(H)}(z)$, $d_L^{(H)}(y)$ (where the upper index H denote the case with Hubble evolution data added) are summarized in Table I, in company with the best-fitting values of Λ CDM parameters. For the Λ CDM model, we use the same dataset, and the best-fitting value of current matter density fraction parameter $\Omega_{m0} = 0.268$, thus, $q_0 = \frac{3}{2}\Omega_{m0} - 1 = -0.598$. The marginalized likelihood distribution of q_0 is also shown in Figure 1 and 2, respectively.

If we use the SNIa data only, we find that the best-fitting values of the deceleration parameter are both negative, which are larger than that of the Λ CDM model, and we can not exclude the case of $q_0 > 0$ even within 1σ error. What's more, the present value of the acceleration rate shows a slight tendency of decrease for the case of y -redshift expansion, compared with the case of redshift expansion. Note that even though the y -redshift expansion is systematically more accurate than the redshift expansion, but the figure of merit (FoM) of q_0 , j_0 and s_0 is smaller, it is 1.10 for redshift expansion and 0.02 for y -redshift expansion. Compared to the redshift expansion, the y -redshift expansion gives a weaker constraint on the snap parameter. Recently, Xia et al. [25] investigated

the fifth order parameter c_0 using the similar cosmographic approach and found that the constraint on it is much weaker.

With the Hubble evolution data added, the constraint ability is stronger, and the FoM for redshift and y -redshift expansion are 3.07 and 0.52, respectively. It worths noting that by employing the FoM to compare the constraint ability of the two methods, one often assumes that the parameters' log-likelihood surface can be quadratically approximated around the maximum, and the likelihood for the data is Gaussian. So, it may significantly mis-estimate the size of the errors if these assumptions do not hold. On the other hand, the Bayesian Evidence, E , provides us with a good method to compare different models [27], which is not dependent on those assumptions. And the ratio of Evidences for two models $B_{12} \equiv E(M_1)/E(M_2)$, also known as the Bayes factor, provides a measure with which to discriminate the models. We calculate the Bayesian Evidence ratio of the redshift and y -redshift expansion methods, and find that for the case of SNIa data used only, $\ln B = -0.83$, while for the case with Hubble data added, $\ln B = -0.37$. It looks that the y -redshift expansion is a bit better. According to the Jeffreys grades, however, the result means that these two expansion methods are comparable in fitting the Union2 dataset. We see from the results that the redshift expansion approach excludes the case $q_0 > 0$ at about 95.4% confidence level, which tells us that the present universe is still in the stage of accelerating expansion. The constraint on the snap parameter is much tighter in the case of redshift expansion, and the constraint ability is improved in some degree with our method compared with some existing studies [13, 25].

It is of interest to investigate the evolution behavior of the deceleration parameter to compare with the Λ CDM model, since different behaviors may tell something on the universe. And another change in the sign of the cosmic acceleration is also interesting to us, if any. Using the best-fitting parameters, the deceleration parameter can be expanded with the redshift and y -redshift, respectively, as

$$q(z) = q_0 - (q_0 + 2q_0^2 - j_0)z + \frac{1}{2}(2q_0 + 8q_0^2 + 8q_0^3 - 7q_0j_0 - 4j_0 - s_0)z^2, \quad (10)$$

parameter	q_0	j_0	s_0	χ^2
$d_L(z)$	$-0.357_{-0.533, -0.58}^{+0.557, +0.57}$	$-1.826_{-4.792, -5.293}^{+5.848, +5.975}$	$-1.878_{-9.468, -13.905}^{+20.484, +21.703}$	524.117
$d_L(y)$	$-0.150_{-0.560, -0.795}^{+0.915, +1.456}$	$-6.564_{-21.400, -26.131}^{+11.119, +14.520}$	$-51.042_{-79.602, -90.412}^{+93.324, +125.622}$	524.086
$d_L^{(H)}(z)$	$-0.403_{-0.338, -0.431}^{+0.318, +0.352}$	$-1.230_{-3.468, -4.374}^{+3.218, +3.676}$	$-2.393_{-4.631, -9.281}^{+6.926, +7.891}$	527.044
$d_L^{(H)}(y)$	$-0.255_{-0.248, -0.445}^{+0.269, +0.460}$	$-7.631_{-6.185, -8.842}^{+5.110, +8.528}$	$-65.741_{-51.988, -80.440}^{+35.462, +72.343}$	528.844
Λ CDM	-0.598	1	-0.206	525.765

TABLE I: The best-fitting values with 1σ and 2σ errors of q_0, j_0 and s_0 . And the best-fitting values of Λ CDM model fitted by the same SNIa data.

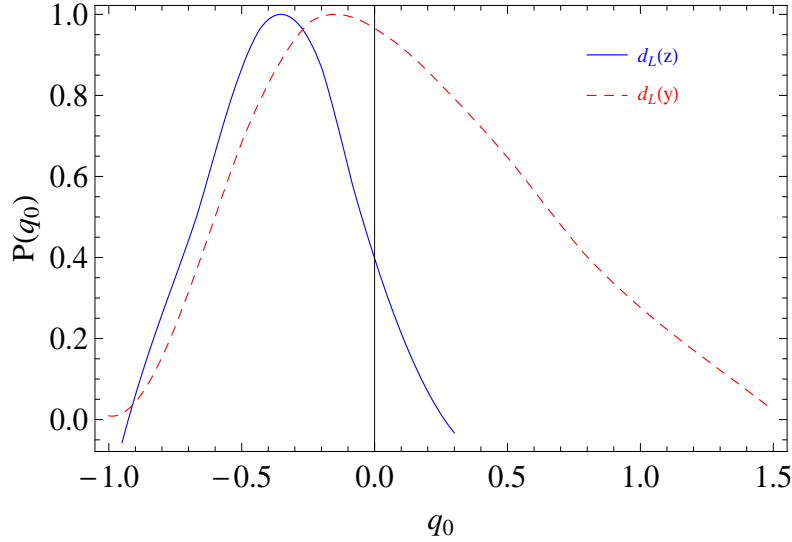


FIG. 1: 1D marginalized distribution probability for the present deceleration parameter from the SNIa data. Curves are scaled to $\max[P(q_0)] = 1$.

and

$$q(y) = q_0 - (q_0 + 2q_0^2 - j_0)y + \frac{1}{2}(4q_0 + 8q_0^3 - 7q_0j_0 - 2j_0 - s_0)y^2. \quad (11)$$

We note that the quadratic form is essential for the detection of the transient acceleration phase, since in this scenario, q should be positive in the past ($z > 2$) and changes its sign at moderate redshift ($z_t \sim 0.3 - 1$), then steps into the phase of $q > 0$. We plot the evolution behaviors of q compared with the Λ CDM model in Figure 3. Because of the weak constraint of the $d_L(y)$, the 1σ area is too large to give any conclusive information,

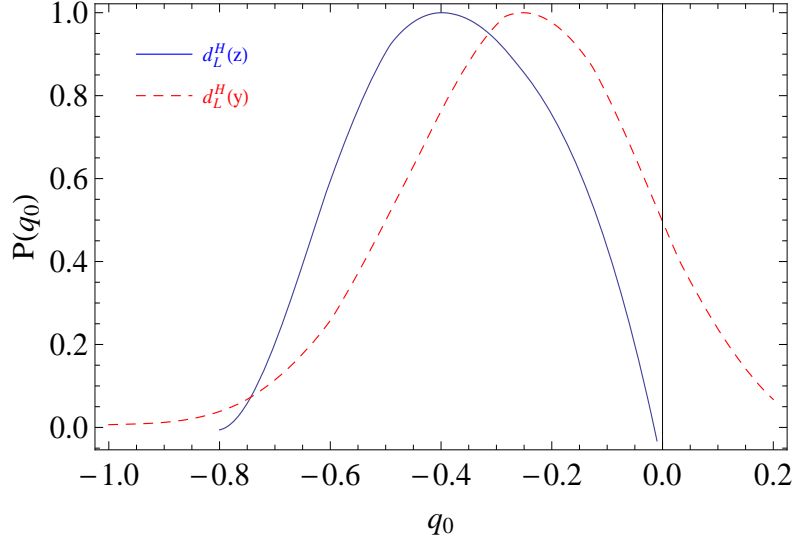


FIG. 2: 1D marginalized distribution probability for the present deceleration parameter from the SNIa data and the Hubble evolution data. Curves are scaled to $\max[P(q_0)] = 1$.

therefore we do not show it here.

The best-fitting curves in the figures show a remarkably different evolution behaviors of the deceleration parameter from the Λ CDM model, all of which indicate a transient acceleration. The Λ CDM model predicts that the universe began to accelerate at $z = 0.35$, but in our analysis, the redshift expansion predicts a earlier transition and the y -redshift expansion predicts the similar transition time as the Λ CDM model. However, all cases indicate a transient acceleration phase and predict a decelerated stage in the near future $z < 0$. This picture is even clear in the case of the y -redshift expansion if both datasets are used, which shows a considerably positive deceleration probability today and in the future, at 68.3% confidence level, and it indicates that the Λ CDM model is completely excluded in the future. The behavior of transient acceleration is also predicted or allowed by several dynamic models [9, 30]. Due to large uncertainties at high redshifts and in the future, however, it is still not able to confirm the existence of transient acceleration phase, nor the future decelerated acceleration, even at 1σ confidence level.

Next, we plot the curves of $E(z)$ for the four cosmographic models and the standard

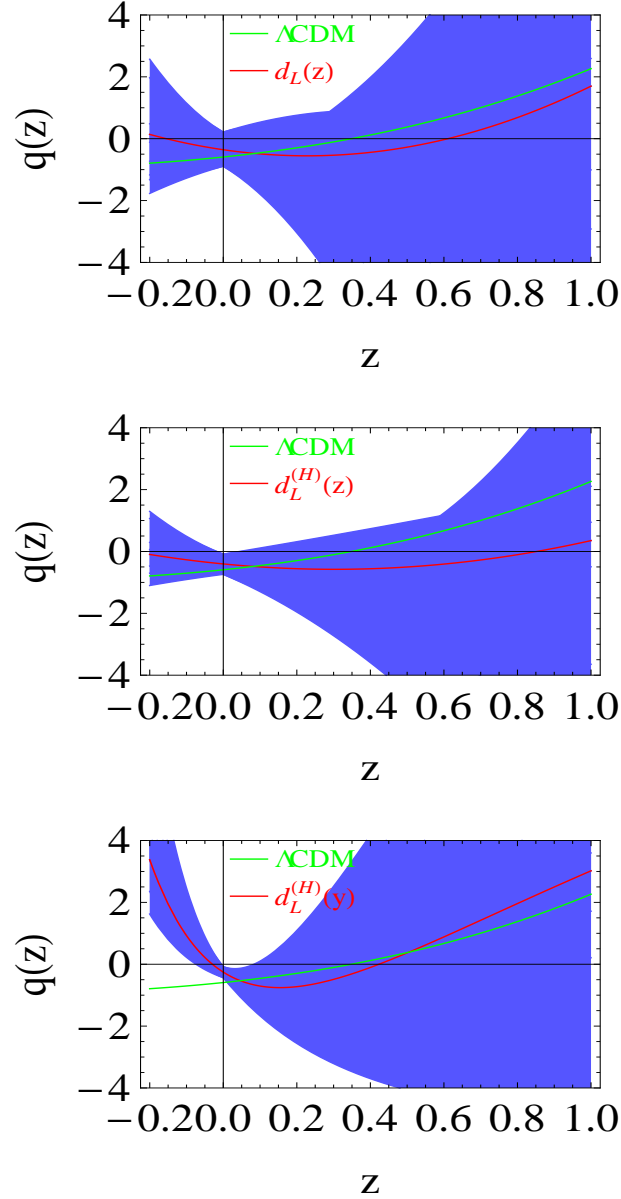


FIG. 3: Evolution behaviors of the deceleration parameter. The red one is the best-fitting curve of $q(z)$ and the green line is the evolution of $q(z)$ derived from the Λ CDM model. The blue area delimits the 68.3% confidence region for the $q(z)$ reconstruction.

Λ CDM model using the best-fitting parameters, compared with the Hubble evolution data in Figure 4. We see from the figure that the curves are all nicely consistent with the data, including the Λ CDM model. The two curves including the Hubble evolution data are much close to the one of the Λ CDM model than the other two. Note that 6 of

the 11 Hubble evolution data have large error bars, with $\sigma(obs) > 10\%$, and the worst data is $\sigma(obs) = 61.86\%$. So, better measured data are in urgent need to make a definite discrimination among different behaviors of our universe.

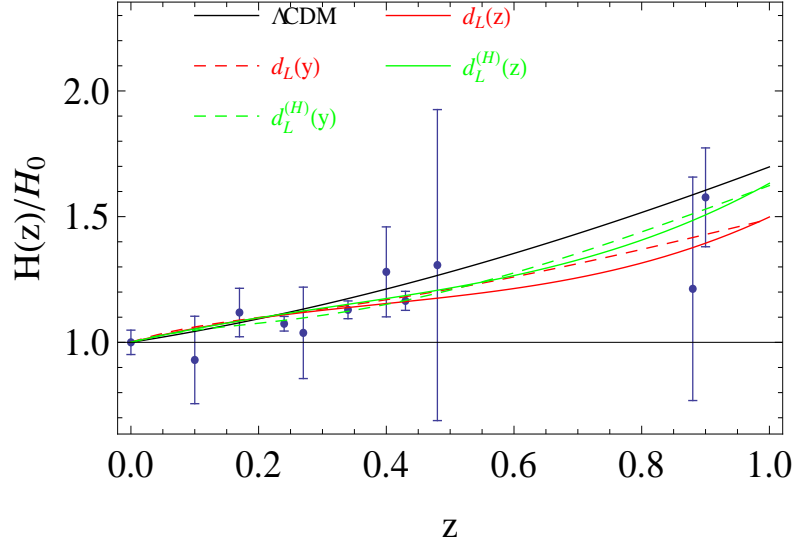


FIG. 4: Best-fitting curves of $E(z)$ derived from the four cosmographic approaches. The red (or dashed red) line denotes the redshift (or y -redshift) expansion using SNIa data only. The green (or dashed green) line denotes the redshift (or y -redshift) expansion constrained with the Hubble data involved. The black one is the evolution of $E(z)$ derived from the Λ CDM model.

III. NON-PARAMETRIZATION APPROACH

Further exploration on the deceleration parameter is also approached with a non-parametrization method, by reconstructing the deceleration parameter from the distance modulus of SNIa directly, which depends neither on the validity of general relativity nor the content of the universe or any assumption regarding cosmological parameters. From mathematics point of view, the determination of the deceleration parameter is much difficult than the evolution of Hubble parameter, since the Hubble parameter is the first order derivative of the comoving distance, while the deceleration parameter is related to

the second order derivative of the comoving distance. And because of that, the error for constructing the deceleration parameter is also larger. To deal with this issue, Ref. [6] generated 2000 artificial data sets mimicking what is expected from SNIa measurement by the SNAP satellite (see [29] or the web site ¹) and then applied the quadratic expansion to express the dimensionless coordinate distance $y(z) = H_0 r(z)$ in each redshift bin, thus the deceleration parameters can be obtained.

There are two sources of errors we try to tackle in the implementation. First, the deviation from the true value of any individual data is assumed to be normally distributed, which is a good approximation only for relatively large samples. Second, any finite dataset, especially small dataset, will contain large sample variance. In summary, smaller number of data produces noisier results, while larger number of data leads to more convictive results at the expense of resolution in larger redshift bins. We try to balance these effects by choosing relatively large number of SNIa data in each redshift bin to make sure that there are both enough data and not too large bins, and also to reduce the effect of sample variance.

In our analysis, we focus on the Union2 dataset instead of the mock datasets and separate the 557 SNIa data equally into four redshift bins, each containing 139 data points (149 data points in the forth bin). In each redshift bin, we reconstruct one data point using the data within each bin, so we get totally 4 reconstructed data, as shown in Table II, where the first column is the averaged redshift in each bin and the third column is the unbiased estimate of the error. We will not take use of the expression of the distance modulus of SNIa, which we believe contains some uncertainties in determining the calibration of the data. Instead, we apply the following expression,

$$\mu_{i+1} - \mu_i = 5 \lg \frac{d_L(z_{i+1})}{d_L(z_i)}, \quad (12)$$

where i runs from 1 to 3 in this case. This expression is credible if the distance modulus is of logarithm form of luminous distance only. In order to detect the deceleration parameter and make it easier for numerical approach, we expand the comoving distance to the second

¹ <http://snap.lbl.gov>

order of redshift in each redshift bin $z_i < z < z_{i+1}$,

$$r(z_{i+1}) = r(z_i) + \frac{1}{H(z_i)} \left[z_{i+1} - z_i - \frac{1 + q_i}{2(1 + z_i)} (z_{i+1} - z_i)^2 \right], \quad (13)$$

where the Hubble parameter can also be expressed with the deceleration parameter,

$$H(z_{i+1}) = H(z_i) \left[1 + \frac{1 + q_i}{1 + z_i} (z_{i+1} - z_i) \right]. \quad (14)$$

And then the luminosity distance can be obtained using the relation $d_L(z) = r(z)(1 + z)$,

$$d_L(z_{i+1}) = \frac{1 + z_{i+1}}{H(z_i)} \left[z_{i+1} - z_i - \frac{1 + q_i}{2(1 + z_i)} (z_{i+1} - z_i)^2 \right] + \frac{1 + z_{i+1}}{1 + z_i} d_L(z_i). \quad (15)$$

For the beginning of the iteration process, we choose $q_0 \approx q_1$. In the following, we will see that this approximation is reasonable since the redshift distance between them is small, with $\delta z = 0.089$. And we use the best-fitting value of Hubble parameter given by the *WMAP7* group, $h_0 = 0.704(km/(s \cdot Mpc))$ [3]. Then we get 3 deceleration parameters, shown in Table III, where we choose the average redshift as the first column. Since $q(z)$ involves the second order derivative of the distance modulus, it is much harder to make the constraint accurately, thus causes the error bars blowing up to be proportional to $(\delta z)^{-5/2}$ [31, 32], similar to the equation of state of dark energy $w(z)$. We plot the evolution of the reconstructed deceleration parameters in Figure 5. As a comparison, other four best-fitting curves of the cosmographic approach are also shown. It is clear that except the Λ CDM model, all other results contain a transient acceleration solution, though the present value of the deceleration parameter is still negative. We cannot discriminate their behaviors at low redshift ($z < 0.4$), but higher redshift behaviors are distinct ($z > 0.6$), thus more accurately detected high- z data are in urgent need. On the other hand, we still need a well behaved method to affirm if there is indeed a transient acceleration phase.

IV. CONCLUSION

To summarize, we have investigate the deceleration parameter in detail, both with the cosmographic approach and the non-parametrization method. These approaches depend

z	μ	σ_μ
0.10286	35.3573	0.1867
0.17760	39.4708	0.1616
0.40451	41.7502	0.2926
0.78596	43.4330	0.3439

TABLE II: Reconstructed distance modulus of Union2 SNIa data, where the first column is the averaged redshift in each bin and the third column is the unbiased estimate of the error.

z	$q(z)$	σ_+	σ_-
0.089	-0.0834	+2.0285	-2.2051
0.291	-2.7717	+3.1068	-1.7184
0.595	2.2651	+1.3969	-0.9106

TABLE III: Reconstructed deceleration parameters of Union2 SNIa data, where the last two columns are the estimates of the errors in each redshift bin, which are also directly constructed from the SNIa data by considering the full error of each data point.

neither on the validity of general relativity nor the content of the universe. To make the results robust, we focus on reducing the systematic error throughout the paper.

Cosmographic approach to detect the deceleration parameter is to expand the luminosity distance to the fourth order or even higher order of redshift or the so called y -redshift, and then to fit the datasets. But this method contains large uncertainties if we use the high- z data. Some authors cut off high- z data in data fitting process to avoid the problem, but we used other technique to reduce the systematic error: By expanding the luminosity distance in two redshift bins which contain the same number of SNIa data, the error can be reduced. Since the deceleration parameter is related to the second order derivative of the luminosity distance, and the first order derivative of the Hubble parameter, it is also necessary to expand the Hubble parameter to the third order as what we have done for the luminosity distance, thus improving the constraint ability. The result reveals that the universe may transit from decelerating expansion to a transient accelerating expansion

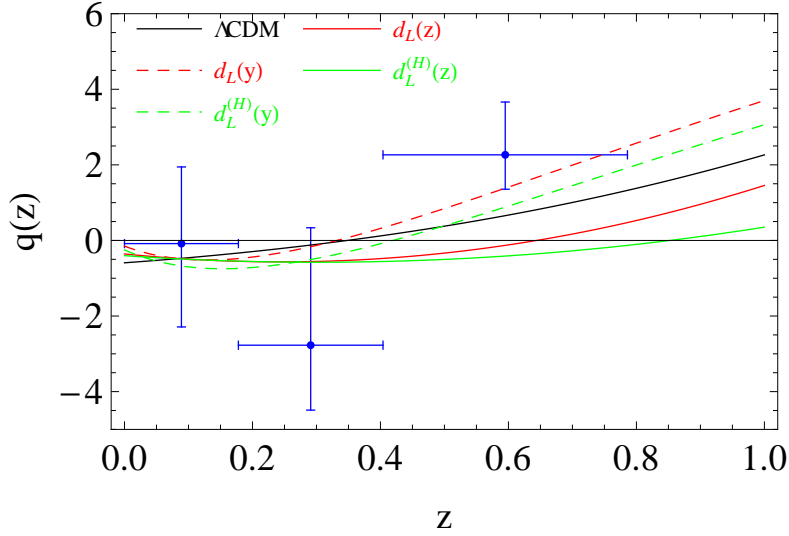


FIG. 5: Evolution of the deceleration parameter reconstructed from the Union2 SNIa data with 1σ error bars. Others are the best-fitting curves of the cosmographic approach as before, in company with that of the Λ CDM model.

during $0.3 < z < 1.0$, and the best-fitting evolution behaviors tell us that it is possible that the universe will return to decelerating expansion stage in the future even though it is still accelerating at present. Comparing with the Hubble data shows that these results are indistinguishable with that of the Λ CDM model, which demands for more accurate observations to come up with a conclusive verdict.

Non-parametrization method is also implemented by reconstructing the deceleration parameters directly from the SNIa data. We simply use the logarithmic form of the distance modulus with respect to the luminosity distance, thus avoid the uncertainties in calibration of the data. To reduce the systematic error, we distribute the same number of SNIa data in each redshift bin to make sure of enough data and not too large width of redshift bin. The result also indicates a transient accelerating expansion stage of our universe. Since the deceleration parameter is much more sensitive to the accuracy of the SNIa data than the Hubble parameter, it is not a easy job to constrain the result tightly, thus needs further improvement, both in observation data and fitting methods.

ACKNOWLEDGEMENTS

ZLT is really grateful to Bin Hu, Qiping Su and Hongbo Zhang for their useful suggestions. RGC thanks the organizers and participants for various discussions during the workshop “Dark Energy and Fundamental Theory” supported by the Special Fund for Theoretical Physics from the National Natural Science Foundation of China with grant No. 10947203. This work was supported in part by the National Natural Science Foundation of China (No. 10821504, No. 10975168, No.11035008 and No.11075098), the Ministry of Science and Technology of China under Grant No. 2010CB833004, and a grant from the Chinese Academy of Sciences.

-
- [1] A. G. Riess *et al.* [Supernova Search Team Collaboration], *Astron. J.* **116**, 1009 (1998) [arXiv:astro-ph/9805201]; S. Perlmutter *et al.* [Supernova Cosmology Project Collaboration], *Astrophys. J.* **517**, 565 (1999) [arXiv:astro-ph/9812133].
 - [2] D. J. Eisenstein *et al.* [SDSS Collaboration], *Astrophys. J.* **633**, 560 (2005) [arXiv:astro-ph/0501171]; U. Seljak *et al.* [SDSS Collaboration], *Phys. Rev. D* **71**, 103515 (2005) [arXiv:astro-ph/0407372].
 - [3] E. Komatsu *et al.* [WMAP Collaboration], *Astrophys. J. Suppl.* **192**, 18 (2011) [arXiv:1001.4538 [astro-ph.CO]]. D. N. Spergel *et al.* [WMAP Collaboration], *Astrophys. J. Suppl.* **170**, 377 (2007). [astro-ph/0603449].
 - [4] V. Sahni and A. A. Starobinsky, *Int. J. Mod. Phys. D* **9**, 373 (2000) [arXiv:astro-ph/9904398];
S. M. Carroll, *Living Rev. Rel.* **4**, 1 (2001) [arXiv:astro-ph/0004075];
P. J. E. Peebles and B. Ratra, *Rev. Mod. Phys.* **75**, 559 (2003); T. Padmanabhan, *Phys. Rept.* **380**, 235 (2003); E. J. Copeland, M. Sami and S. Tsujikawa, *Int. J. Mod. Phys. D* **15**, 1753 (2006); M. Li, X. D. Li, S. Wang and Y. Wang, *Commun. Theor. Phys.* **56** (2011) 525 [arXiv:1103.5870 [astro-ph.CO]].
 - [5] Y. Wang and M. Tegmark, *Phys. Rev. D* **71**, 103513 (2005) [arXiv:astro-ph/0501351].
 - [6] R. A. Daly and S. G. Djorgovski, *Astrophys. J.* **597**, 9 (2003) [arXiv:astro-ph/0305197];

- R. A. Daly and S. G. Djorgovski, *Astrophys. J.* **612**, 652 (2004) [arXiv:astro-ph/0403664].
- [7] J. Barrow, R. Bean and J. Magueijo, *Mon. Not. Roy. Astron. Soc.* **316**, L41 (2000) [arXiv:astro-ph/0004321].
- [8] M. Chevallier and D. Polarski, *Int. J. Mod. Phys. D* **10**, 213 (2001) [arXiv:gr-qc/0009008].
R. R. Caldwell and E. V. Linder, *Phys. Rev. Lett.* **95**, 141301 (2005) [arXiv:astro-ph/0505494].
- [9] A. Shafieloo, V. Sahni and A. A. Starobinsky, *Phys. Rev. D* **80**, 101301 (2009) [arXiv:0903.5141 [astro-ph.CO]].
- [10] Y. G. Gong, B. Wang, R. G. Cai, *J. Cosmol. Astropart. Phys.* **04**, 019 (2010);
- [11] Z. Li, P. Wu and H. Yu, *Phys. Lett. B* **695**, 1 (2011) [arXiv:1011.1982 [gr-qc]].
- [12] S. Nesseris and L. Perivolaropoulos, *JCAP* **0702**, 025 (2007) [arXiv:astro-ph/0612653].
- [13] M. V. John, *Astrophys. J.* **614**, 1 (2004); M. Visser, *General Relativity and Gravitation* **37**, 1541 (2005); C. Cattoen, M. Visser, *Phys. Rev. D* **78**, 063501 (2008); M. Visser, *Class. Quant. Grav.* **21**, 2603 (2004); M. V. John, *Astrophys. Space Sci.* **330**, 7 (2010).
- [14] A. C. C. Guimaraes, J. V. Cunha and J. A. S. Lima, *JCAP* **0910**, 010 (2009) [arXiv:0904.3550 [astro-ph.CO]];
J. V. Cunha, *Phys. Rev. D* **79**, 047301 (2009);
- [15] Y. Gong, A. Wang, *Phys. Rev. D* **75**, 043520 (2007).
- [16] A. C. C. Guimaraes and J. A. S. Lima, *Class. Quant. Grav.* **28**, 125026 (2011) [arXiv:1005.2986 [astro-ph.CO]].
- [17] P. Wu and H. W. Yu, arXiv:1012.3032 [astro-ph.CO].
- [18] C. Cattoen and M. Visser, *Class. Quant. Grav.* **24**, 5985 (2007) [arXiv:0710.1887 [gr-qc]].
- [19] R. Amanullah *et al.*, *Astrophys. J.* **716**, 712 (2010) [arXiv:1004.1711 [astro-ph.CO]].
- [20] C. Cattoen, M. Visser, *Classical and Quantum Gravity* **24**, 5985 (2007).
- [21] S. Capozziello, R. Lazkoz and V. Salzano, arXiv:1104.3096 [astro-ph.CO].
- [22] D. Stern, *et al.*, *J. Cosmol. Astropart. Phys.* **02**, 008 (2010).
- [23] E. Gaztanaga, A. Cabre and L. Hui, *Mon. Not. Roy. Astron. Soc.* **399**, 1663 (2009) [arXiv:0807.3551 [astro-ph]].
- [24] S. Weinberg, *Cosmology and Gravitation*, John Wiley Sons, New York (1972).

- [25] V. Vitagliano, J. Q. Xia, S. Liberati, M. Viel, JCAP **3**, 5 (2010); J. Q. Xia, V. Vitagliano, S. Liberati and M. Viel, arXiv:1103.0378.
- [26] A. G. Riess, *et al.*, Astrophys. J. **699**, 539 (2009).
- [27] Jeffreys H., Theory of Probability, Oxford University Press, Oxford (1961).
- [28] S. Nesseris and L. Perivolaropoulos, Phys. Rev. D **72**, 123519 (2005)
- [29] G. Aldering *et al.* [SNAP Collaboration], arXiv:astro-ph/0209550.
- [30] F. C. Carvalho, J. S. Alcaniz, J. A. S. Lima and R. Silva, Phys. Rev. Lett. **97**, 081301 (2006) [arXiv:astro-ph/0608439].
- [31] M. Tegmark, Phys. Rev. D, **66**, 103507 (2002).
- [32] M. Tegmark, D. J. Eisenstein, W. Hu, R. G. Kron, [astro-ph/9805117].